Design and Experimentation of a Wireless Sensor Network Node Powered by Vibration Energy

Yek Hong Tham
School of Engineering and Computer Science
Victoria University of Wellington
Wellington 6140, New Zealand
Email: Yek.Tham@xtra.co.nz

***Abstract*—The limitation of wireless sensor networks (WSN) that operate by harvesting ambient energy is the scarcity of electrical energy generated to run embedded applications over the woken period. The novelty using the power source as a sensor of a wireless sensor node reduces energy consumption and provides a low cost solution for the application of detecting vibrations. While harvesting the mechanical energy from the tremor event, the wireless sensor node uses the energy harvesting behavior to be interpreted into vibration measurements, thus we have a simple and yet elegant design. In order to prove this design concept, a prototype was built in order to demonstrate the energy harvesting and sensing ability and to measure the performance of the prototype in terms of power utilisation and packet transmission rate.**

Keywords-Wireless Sensor Networks (WSN); Vibration; Energy Harvesting; IEEE802.15.4;

I. INTRODUCTION

A Wireless Sensor Network (WSN) consists of spatially distributed autonomous sensors (referred to as 'nodes') that monitor physical conditions such as temperature, sound vibration, pressure, etc. and transfer the detected data along nodes in the network to a target location. They allow monitoring and controlling capabilities in such industries such as transportation, environmental oversight, safety and security and military [1]. Each node will consist of a processing capability with storage capability, radio frequency transceiver, power source and peripheral sensors or actuators [2]. Wireless sensor nodes are often deployed in decentralised types of networks that do not rely on pre-existing infrastructures such as routers and operate in real-time with limited power source.

WSNs that are powered from non-traditional sustainable sources has become increasingly important due to the growing environmental concerns to conserve energy. Traditionally WSNs were powered from batteries however batteries have a limited operating lifetime and the energy source would need to be replenished by replacing the battery on an expected timely basis incurring additional cost for maintenance and could sometimes be cumbersome or infeasible such as where a node may be embedded in a concrete building or a location that is humanly impossible to reach. Also the contents of the battery can leak and create a problem that may cause the node to fail [3].

The issues arising from using traditional methods of powering WSNs as well as the motivation to conserve energy has led to the option of harvesting ambient from the environment to power the WSNs.

II. DESIGN

The wireless sensor node design was abstracted into four main components; the energy harvesting unit, the power management unit, the central processing unit and the radio transceiver unit. Each subsystem will be described in detailed in their respective

sections. The novelty of the design was not to include a dedicated sensor unit instead the energy harvesting unit was employed to act as a sensor as well as a power source to perform packet transmissions. The rate of packet transmission can be translated into vibration information and thus taking care of the sensor.

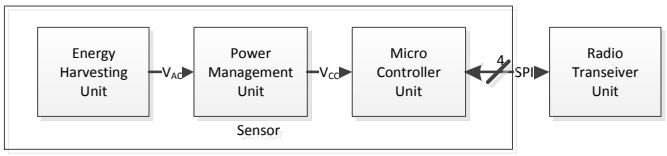

Figure 1

A. The Energy Harvesting Unit

The energy harvesting unit employed was a MIDE's V25w Piezoelectric Vibration Energy Harvester. The energy harvesting unit was a piezoelectric transducer in the form of a cantilever with a stack of two piezoelectric elements where the material is industrial standard Lead Zirconate Titanate (PZT-A5) [4][5]. Simply put, when there is mechanical stress in the piezoelectric element deforms the crystal lattice and the charges within the lattice is disturbed which is capable of creating a large potential difference, with trivial amounts of current.

In the event where the piezoelectric transducer experiences a vibration, the amount of energy that is harvested is depended on the frequency and amplitude of the event. Therefore the piezoelectric transducer must be tuned to a resonant frequency that is matched with the natural frequency of the event to achieve maximum power output. The author of a related research document [6] states how tuning the piezoelectric transducer is achieved:

"For tuning purposes, it is enough to know that the resonance frequency of the device is decreased either by increasing the weight used on the cantilevered beam or increasing the distance of the weight from the fixed end of the beam".

There are three considerations that influenced the output of the wireless sensor node and that was the frequency the cantilever oscillation, the duration of the event and the magnitude of the event which in turn determines the amplitude of the vibrating cantilever. It is desirable for the piezoelectric transducer to be tuned to low frequencies for the applications of monitoring low frequency high acceleration tremors such as earthquakes. Earthquakes are known to occur with a frequency range of 0.1 Hz to 20 Hz [7].

B. The Power Management Unit

The power management system was a MIDE's EHE004 Energy Conditioning Circuit. The EHE004 has a LTC3588-1 integrated circuit which integrates a full-wave bridge rectifier to convert the AC voltage generation from the energy harvesting unit into DC and a buck converter to step down the harvested high voltage (high voltage is typical in piezoelectricity) to a lower operable voltage [8].

One notable point to mention is that the circuit had a built in hysteresis mechanism which allowed the reservoir capacitor to charge, without the hysteresis mechanism a problem would occur at the instance the capacitor begins to charge the buck converter would attempt to convert the charge stored in the capacitor prematurely rendering the storage capacitor useless. The wider the hysteresis window the greater amount of energy can be stored.

The charge management circuit employs a 200µF (two 100µF in parallel) Niobium Oxide capacitor to store charge. Niobium Oxide capacitors share similar characteristics to tantalum capacitors in terms of small packaging size, low current leakage and better temperature stability compared to Aluminum Electrolytic capacitors. However one benefit with Niobium Oxide capacitor is

that when a Niobium Oxide capacitor fails, it fails in a safe fashion where it develops high resistance after breakdown unlike Tantalum or Aluminum Electrolytic capacitors which develop low resistance and shorts the circuit [9].

The energy management device has three configurable mechanisms; Piezo connection, DC output setting and rectification method. The piezo connection can be configured in either series or parallel, the piezoelectric is stacked in a bimorph configuration (two active layers of PZT piezoelectric layer and metal layer), the series piezo configuration connects the two piezo elements in series allowing twice the voltage at a lower current being generated and in parallel would result in twice the current at a lower voltage generation. MIDE recommended that at lower vibrations where voltage generated is small the series connection would be a suitable configuration of the piezoelectric elements. The DC output setting configuration allows for possible regulated DC outputs; 1.8 V, 2.5 V, 3.3 V, and 3.6 V. All DC voltage levels are suitable for powering the wireless sensor node. The rectification method can be configured in normal mode which utilises the full-wave bridge rectifier of the charge management IC and the superseries mode where the bridge rectifier of the charge management IC is configured to a half-wave bridge configuration. The difference between the two configurations is that the output voltage of the full-wave bridge rectifier is half the peak-to-peak input voltage minus two voltage drops (400 mV) and for the half-wave bridge rectifier there is only one diode drop (200 mV).

C. The Microcontroller Unit

Selecting a microcontroller with low power consumption was important because the energy harvesting unit harvests energy at a relatively low rate. From surveying what low power microcontroller the MSP430 family of Texas Instruments (TI) and ATmega 8-bit family of Atmel Corporations are used in wireless sensor networks [10]. The MSP430 family had the best performance in terms of power consumption and has a large community with support for many low power applications. The MSP430 family has different types of microcontroller and hence the guide [11] provided by TI was used to select desired MSP430 microcontroller. The MSP430F2618 was the chosen microcontroller because the material provided with this microcontroller made the development process simpler, specifically speaking, there was already an 802.15.4 library written for the MSP430F2618 by TI and also the CC2520 transceiver datasheet [12] provides routing details between the microcontroller and the CC2520 transceiver.

The summarized specifications of the microcontroller are shown in Table 1 from [10].

MSP430F2618	
Specification	**Value**
Supply Voltage	1.8-3.6V
Maximum Operating Frequency	16 MHz
RAM	8 KB
Flash	116 kB
On-Chip Peripherals	Watch Dog Timer, dual 12-bit DAC, 12-bit ADC, dual 16-bit timer, three-channel DMA, four USCIs, hardware multiplier
Active Current	0.365 mA at 1MHz, 2.2V
Standby Current	0.5 μA
Off Current	0.1 μA

Table 1

D. The Radio Transceiver Unit

The TI CC2520 was selected to RF connectivity based on the IEEE 802.15.4 standard. The features of the transceiver listed in the datasheet specify a 400 metre line-of sight range, a supply voltage range of 1.8 V to 3.8V and a link budget of 103dB [12]. The Power specifications of the transceiver are shown in Table 2.

The CC2520 interfaced with the microcontroller via the 4-wire Serial Peripheral Interface (SPI) bus. The SPI interface provided synchronous full duplex communication consisting of three lines active low; Chip Select (CSn), Serial Clock (SCLK) and Serial In (SI) as input lines to the slave device (CC2520 transceiver) that were used as a reset signal, provide timing for synchronous communication in duplex mode and transmitting serial data. The fourth line Serial Out (SO) was used to transmit data from the transceiver to the master device which was the microcontroller.

CC2520	
Specification	**Value**
Supply Voltage	1.8-3.8V
Interfer Frequency	2400 MHz
Output Max Power	+5 dB
Receiving Sensitivity	-98 dBm
Transmitting Current	33.6 mA at 5dBm 25.8 mA at 0dBm
Receiving Current	18.5 mA at -50dBm
Sleeping Current	0.12 µA

Table 2

III. IMPLEMENTATION

The microcontroller had an internal digital control oscillator (DCO) operating at 1 MHz which was the lowest configurable frequency. Initially an external low-frequency 32768 Hz watch Crystal Oscillator (henceforth referred to as XOSC) was to serve as the main oscillator for the microcontroller in attempts to operate at a lower power because one application note [13] stated that the 32768 Hz XOSC consumed little power because of its low generated frequency. The use of a 32 kHz watch crystal had led to the problem of failing to transmit the first packet and intermittently failing to transmit intermediate packets as well. This was due to the start-up time taken for the XOSC which varied between several hundred milliseconds and a few seconds for low frequency XOSCs like the 32768 Hz XOSCs. This meant that there was not enough energy stored in the reservoir capacitor for the stabilisation of the crystal oscillator resulting in intermittent transmission failures. To solve this problem the internal RC oscillator was used instead as the clock source driving the DCO to synthesise the 1 MHz frequency for the microcontroller.

Although the datasheet specified that both the transceiver chip and the microcontroller chip can function at the minimum operating voltage 1.8 V however the wireless node was not able to transmit a packet when the DC output setting of the power management device was configured to 1.8 V output. When the DC output setting of the device was set to 3.6 V the highest the wireless sensor node was then able to transmit a packet. The reason behind the failure at low voltage was due to duration of the initial start-up. With a lower voltage the duration to start-up the microcontroller and transceiver would take longer. And when the XOSC was used the start-up was long to complete the transmission with the available energy capacity. When the internal RC oscillator was used instead of the XOSC the operating voltage was left at 3.6 V to achieve the best possible start up time.

The microcontroller was programmed in ISO C in Code Composer Studio which is an IDE that was based on the Eclipse open source software framework. A simple program was written to verify that it was possible to send a packet with the available energy capacity. It was important to have minimal code and avoid loops as more instructions results in a longer execution.

The code's function is summarised in Figure 2.

1. Initialise the microprocessor.
2. Initialise the SPI interface.
3. Construct the members of the packet header (Destination PAN, Destination Address, Source Address etc)
4. Initialise the RF transceiver.
5. Write something to the payload.
6. Send the packet.

Figure 2

Once all instructions are executed the remaining energy is wasted as the microcontroller is idle in active mode, i.e. the remaining energy is used to power the internal clock module of the microcontroller while not performing any instructions.

Since the piezoelectric energy harvester generates an AC voltage. It must be converted into DC though a full-wave bridge rectifier. The LTC3588-1 charge management device contains an internal full-wave bridge rectifier which can be configured in a full-wave or half-wave mode via the 'rectification method' mechanism implemented in the EHE004. It is desirable to produce energy from the smallest vibration possible so the rectification method was set to half-wave rectification. A half-wave rectifier will only loose energy from one diode drop as oppose to two voltage drops if it were to operate in a full-wave rectification mode.

When the capacitors are fully charged then the buck converter is triggered to step down the voltage stored in the capacitor. Equation (1) shows the approximate formula for calculating the average energy stored in the reservoir capacitor based on the voltage hysteresis window of the EHE004. The average power dissipation can be determined from the microcontroller datasheet using the current values in active mode. The voltage hysteresis high-point in which the buck converter is activated is 5.04 V and once triggered the voltage stored in the capacitor is discharged down to 4.03 V, by using the formula in Equation (1), one can calculate the energy capacity available for a transmission operation over the woken period.

$$E = {}^{1}/_{2}\, C|V_f - V_i|^2 \qquad (1)$$

IV. Performance Evaluation

A. Evaluating Power

The power output of the piezoelectric element was measured while connected to a full-wave diode rectifier and capacitor load of 10 µF. The piezoelectric element was mounted on the shaker with the 40g tungsten mass so that the resonant frequency of the cantilever was 7 Hz to which equal the frequency that the shaker was vibrating at. The amplitude of the shaker was varied and a digital multimeter was used to capture the voltage across the capacitor over time. The energy stored in the capacitor can be calculated Equation (2) and divided by the time to reach full charge capacity to determine the rate of energy output, i.e. power.

$$P_{AVG} = \frac{{}^{1}/_{2}\, C|V_f - V_i|^2}{\Delta t} \qquad (2)$$

1) Average Power vs. Amplitude

Figure 3 shows the average power output from the piezoelectric element at various amplitudes in the units of root mean square gravitational acceleration. Current was then later derived from the power values by measuring the resistance of the wire connected to the capacitor load. Figure 4 shows the average current derived from the measurements of Figure 3.

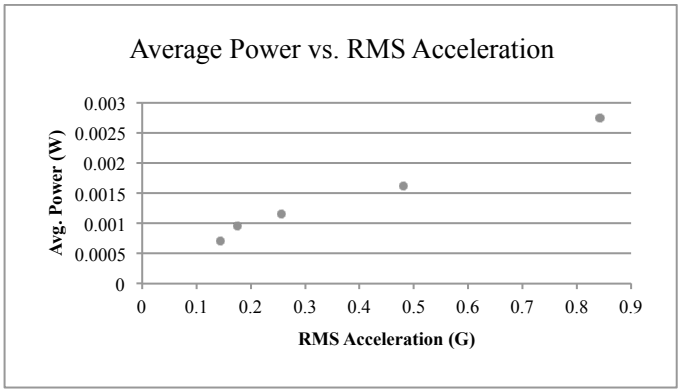

Figure 3

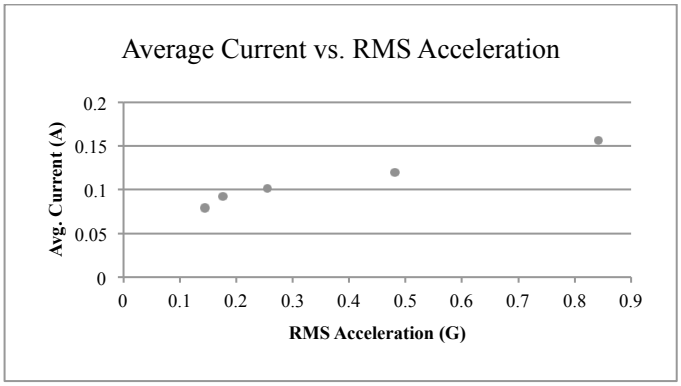

Figure 4

2) Packet Burst Limit & Power Utilisation

The packet burst limit measured how many packets once woken execution could send which provided an approximation to the energy consumption just transmitting a packet (with a payload length of 1 byte and excluding startup consumption). The peak capacity limit was measured by calling the function for Step 6 in Figure 2 within a do-while-true loop. The minimum packet burst limit was 5 packets, which definite with amplitudes below 0.2 G and The maximum packet burst limit was 6 packets when higher than 0.2 G. Using Equation (1) the energy required to send a packet was calculated to be 0.15 mJ to 0.18 mJ. This was verified through measurement of the current using a digital multimeter with a sample rate of 100 µs. In Figure 5 the current consumption was measured over time and two large pulses are observed, the first pulse between the 0 s and 0.002 s represents the start-up power consumption and later between 0.012 s and 0.014 s another pair of pulses represented the power on transceiver and transmission of the packet, the area under the curve between 0.012 s and 0.014 s confirmed the energy consumption for transmitting a packet.

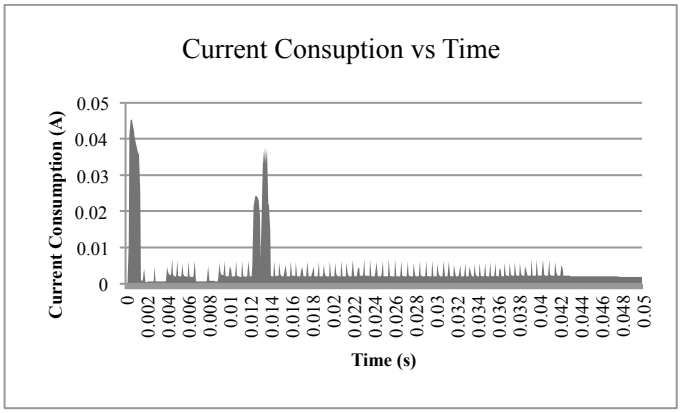

Figure 5

B. Evaluating Functionality

1) Charging Time for First Packet Transmission

Initially there was no charge stored in the capacitor therefore the time needed to send the first packet will be longer than the subsequent packets in a transmission event. It was necessary to measure how long it would take to send the initial packet of a transmission stream. Figure 6 shows the initial delay required to transmit the first packet.

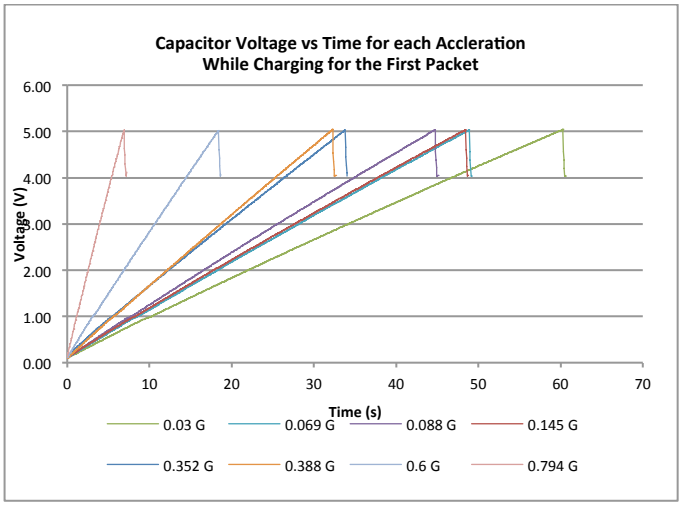

Figure 6

2) Transmission Interval vs. Vibration Amplitude

The average transmission interval was measured as the amplitude was varied. The unit of measure of the amplitude is the root mean square acceleration, G, (1 G = 9.81 ms^{-2}) rather than displacement of the shaker platform. The shaker was used to establish the parameters amplitude and frequency to simulate the event.

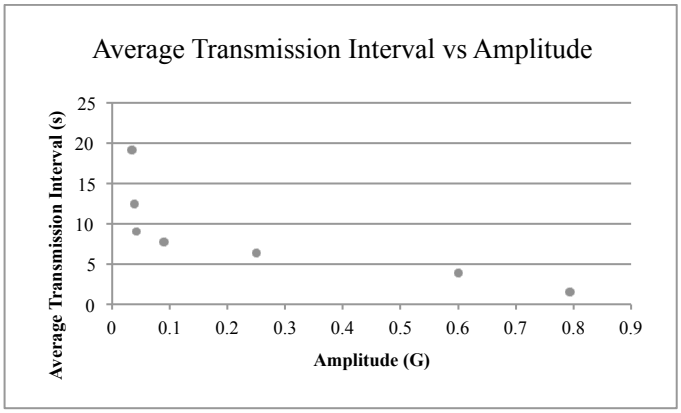

Figure 7

The chart in Figure 7 shows that there is some correlation between the average transmission interval and the vibration amplitude. Therefore a transfer function can be derived to translate the transmission interval into vibration amplitude.

3) Transmission Interval vs. Vibration Frequency

If the frequency of the environment is the same as the resonant frequency of the energy harvester then maximum energy rate output is achieved. In all other cases where the vibration frequency of the environment is not resonant the energy rate output is crippled. The next set of measurements show the crippling effects of the shaker not vibrating at resonant frequency and is represented in delay in packet outputs. Note that because RMS acceleration was a function of frequency, the amplitude that was fixed was a displacement of 5 mm.

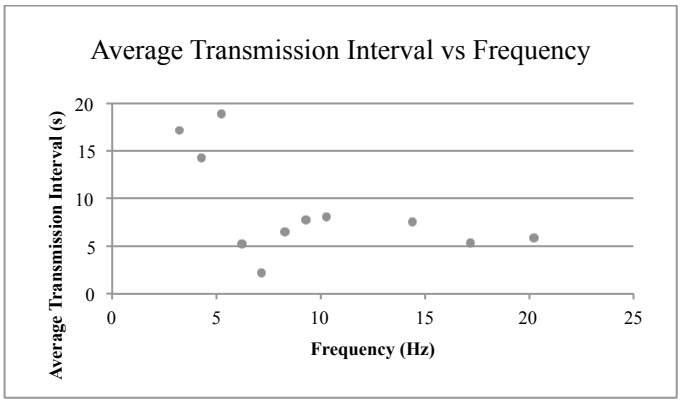

Figure 8

4) Initial Packet Transmission Delay

Initially there is no charge stored in the capacitor therefore the time needed to send the first packet will be longer than the subsequent packets in a transmission event. It was necessary to measure how long it would take to send the initial packet of a transmission stream.

CONCLUSION

The outcome of the design and implementation was a functioning WSN node. The main limitation of the design is the energy harvester is only efficient when the event is vibrating at resonant frequency and in a practical situation the event of a tremor may not vibrate at the desired resonant frequency. If the event was a vibration at a certain fixed frequency then the delay between packets would accurately reflect the amplitude of the vibration.

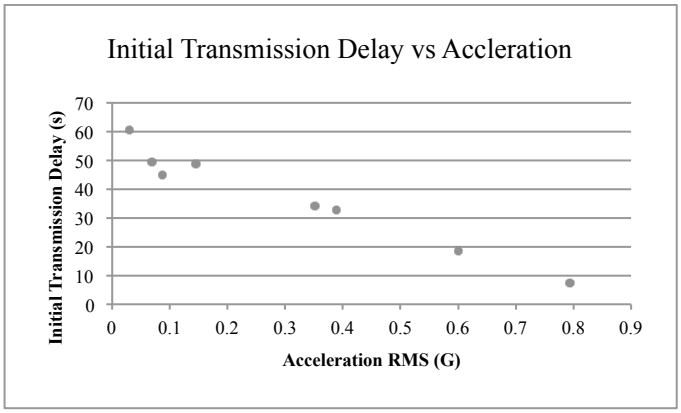

Figure 9

The payload size of the IEEE802.15.4 standard has a maximum payload size of 127 octets, the measured transmission interval difference between sending 1 octet and 127 octets was on the order of 0.01 milliseconds however the integrity of this measurement was subjective because the packet transmission interval noise was larger.

The node can be optimised to reduce the delay between packets with strategies such as reducing the capacitor size where capacitor values must be optimally selected to balance the energy storage capacity against the charging time. Also the remaining stored energy can be discharged through an LED. This may not be necessary if the capacitor value is optimised so that there is not idle time in the CPU. It would even be more efficient if the remaining energy can be fed back to the storage capacitor.

REFERENCES

[1] Pottie. G. J, Kaiser. W. J. W, "Wireless integrated network sensors," Communications of the ACM, vol. 43, No. 5, pp. 51, May 2000.

[2] Stankovic J. A., Wireless Sensor Networks, University of Virginia, 2006, pp.1.

[3] Seah W. K. G, Olds J. P, "Wireless Sensor Networks powered by RF Energy Harvesting: Design and Experimentation," Technical Report No. 12-06, Victoria University of Wellington, Wellington, New Zealand.

[4] Mide Technologies, "QuickPack Frequently Asked Questions," 2012, http://www.mide.com/products/qp/qp_piezo_faq.php

[5] Mide Technologies, "Volture Products - Material Properties," 2012, http://www.mide.com/pdfs/volture_material_properties_2010.pdf

[6] Raj P. S, "Vibration Energy Harvesting using PEH25W," Summer Internship Report, pp. 10, 2011.

[7] Aldasouqi I, Shaout A, "Earthquake Monitoring System Using Ranger Seismometer Sensor," International Journal of Geology, Issue 3, vol. 3, 2009.

[8] Mide Technologies, "EHE004 Energe Harvesting Electronics Datasheet," 2012, http://www.mide.com/pdfs/volture_EHE004_Datasheet.pdf

[9] Zedníček T, "New Tantalum Technologies Tantalum Polymer and Niobium OxideCapacitors," AVX Czech Republic, pp. 4

[10] Peng Y, Luo Q, Peng X, "The Design of Low-power Wireless Sensor Node," Harbin Institute of Technology, Harbin, China.

[11] Texas Instruments Incorporated, "RF Connectivity with TI Microcontrollers," 2011, http://www.ti.com/lit/ml/spab089/spab089.pdf

[12] Texas Instruments Incorporated , "CC2520 Datasheet 2.4 GHz IEEE 802.15.4/Zigbee® RF Transceiver," December 2007.

[13] Energy Micro, "Oscillator Design Considerations AN0016 - Application Note," 2010, available online from: http://downloads.energymicro.com/an/pdf/an0016_efm32_oscillator_design_considerations.